Energy efficient multiejector CO_2 cooling system for high ambient temperature

Simarpreet Singh[(a)], Prakash M. Maiya[(a)], Armin Hafner[(b)], Krzysztof Banasiak[(b)], Petter Neksa[(c)]

[(a)]*Indian Institute of Technology Madras, India*

[(b)]*Norwegian University of Science and Technology, Norway*

[(c)]*SINTEF Energy Research, Norway*

Abstract

Experimental evaluation of a multiejector CO_2 cooling system of 33 kW cooling capacity is conducted for an Indian supermarket at high ambient temperature context. The test-rig is designed to depict the actual supermarket cooling requirements in India with three different cooling temperature levels simultaneously; freezing, medium refrigeration and air-conditioning. The rig is equipped with a novel design consisting of two multiejectors; low ejection ratio ejector (LERE) and high ejection ratio ejector (HERE), in a series configuration. It is observed that the maximum pressure lift of 5.5 bar is obtained with this new design. Moreover, improvement in the overall system performance with the support of the internal heat exchanger (IHX) is evaluated. Enhancements observed in the maximum COP and PIR are 7.2% and 6.2% respectively. Furthermore, the test-rig performance with the flooding and non-flooding of the medium temperature evaporator (refrigeration) is evaluated. It is observed that the evaporator flooding reduces its superheat at the exit by 83.84%, leading to the overall reduction of PIR by 6.51%. The performance of the proposed system is also compared with the reported field data obtained at a low ambient temperature context. The results projected that the proposed cooling system with series multiejector configuration is a reliable choice for higher ambient temperatures and it is expected to outperform the existing systems at lower ambient temperatures.

Keywords: Trans-critical; IHX; Flooding/non-flooding; PIR; Liquid ejector.

1. Introduction

"Nowadays, fluorinated refrigerants appearing in the limelight due to the immediate necessity in ozone layer depletion applicant and global warming causing refrigerants (Calm, 2002). Moreover, such refrigerants can cause several other health issues, for instance, Freon; is an almost odourless

This is the accepted version of an article published in Thermal Science and Engieering Progress
http://dx.doi.org/10.1016/j.tsep.2020.100590

and tasteless gas which after inhaling could cut-off the oxygen supply form the human body, moreover, it results in refrigerant poisoning and a large amount of the same could lead to death (Bhatkar et al., 2013). Conventional refrigerants are quite popular and adopted in developing countries (such as India), for various HVAC&R applications, which not only have a high global warming potential (GWP) but also possesses, concerning level of ozone depletion potential (ODP)".

Figure 1 shows comparison between GWP of a few conventional refrigerants and natural refrigerant CO_2. It is clear from this figure that CO_2 has a definitive advantage over conventional refrigerants in the context of GWP, however the expansion losses during the throttling process in the CO_2 cycle is the reason of lower performance at high ambient temperature conditions. Nevertheless, with realization of the hazardous nature of the synthetic refrigerants, CO_2 is once again gaining popularity as a refrigerant (Lorentzen, 1994). Extensive research has been done on exploring the possible methods to enhance the performance of CO_2 cooling systems for various ambient temperature conditions. Since CO_2 is a by-product of the chemical industry that is normally released into the atmosphere, using it as a refrigerant will add another step before the inevitability (Sawalha, 2008). In addition, CO_2 is non-flammable and non-toxic, thereby making it a suitable alternative for the synthetic refrigerants especially in applications where large amount of refrigerant is needed (Kim et al., 2004).

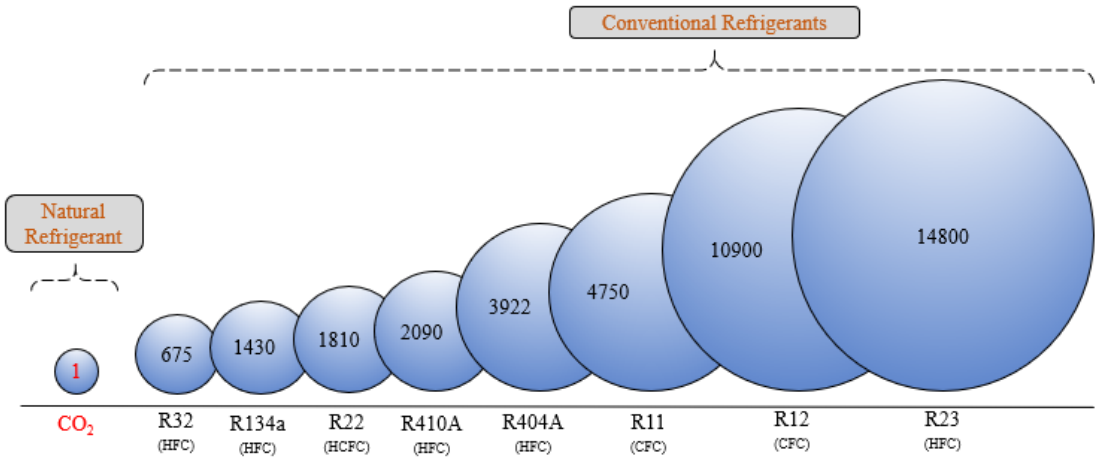

Figure 1. Comparison between GWP of a few conventional refrigerants and natural refrigerant CO_2.

This is the accepted version of an article published in Thermal Science and Engieering Progress
http://dx.doi.org/10.1016/j.tsep.2020.100590

Apart from the environmental concern of constant enhancement in the global warming, energy demands all over the world are also rapidly growing especially in developing countries (Singh and Dasgupta, 2017). Improving the energy efficiency of the cooling systems which are an integral part of services, that are necessary for everyday life could greatly impact the sustainability of the future (Milazzo and Mazzelli, 2017). By designing systems which consume less energy, the emissions can be reduced and the energy savings may result in a reduction of future power plants and other cost of heavy infrastructure associated with it (Dai et al., 2009). A versatile application such as a cooling unit for a supermarket requires various levels of temperatures and the supermarket cooling demand is also rising very rapidly. The operating pressure and temperature characteristics demand a special design for this kind of systems. However, it also offers advantages such as low reduction in saturation temperature for a given pressure drop (Taylor et al., 2007).

In many supermarkets across the world, installed at high ambient temperature regions possesses higher Coefficient of Performance (COP) than the HFC systems during 90% of the operational time in a year (Milazzo and Mazzelli, 2017). Therefore, it makes CO_2 refrigeration an attractive choice for various applications including, beverage cooling cabinets and vending machines. When, not utilizing the high temperature lift potential of the gas cooler and applying expansion work recovery, CO_2 units, might be less energy efficient in high ambient temperature regions when compared to systems which use CFCs and HCFCs (Kim et al., 2004). Several modifications for the conventional cycle have been proposed, including the use of an expander, ejector, etc. in place of the throttle valve in order to retrieve some of the energy that is lost during the expansion (Sharma et al., 2014). However, the use of an ejector has grabbed most attention because of its unique attributes which include low cost, high expansion work recovery potential, absence of moving parts, etc. (Banasiak et al., 2015a). The two-phase ejectors were designed solely based on experiments, but Keenan in 1950 presented one of the first analytical theories based on gas dynamics equations for the perfect gases along with the conservation laws for mass, momentum and energy, disregarding the losses due to heat transfer and friction (Liu and Groll, 2013).

Shifting completely towards the ejector expansion cycle, the dynamic characteristics of systems can be retained and control of the high side pressure based on varying load can also be smoothly performed as reported (Banasiak and Hafner, 2013). Nowadays the ejector technology is very popular for developing cooling racks for supermarket refrigeration (Banasiak et al., 2015b).

This is the accepted version of an article published in Thermal Science and Engieering Progress
http://dx.doi.org/10.1016/j.tsep.2020.100590

Various studies report noticeable advance in the overall system performance. This allows CO_2 to be a viable competitor to the conventional synthetic refrigeration systems globally. However, very limited studies are reported with the use of multiejector in parallel and series configuration design. Moreover, zero superheat at the evaporator exit concept is encouraged to improve the overall performance because IHX is necessary in the CO_2 cycle (Kim et al., 2017). Improvement in the overall performance of the CO_2 system with internal heat exchanger (IHX) is also reported in various studies for different climatic conditions (Goo et al., 2005; Nakagawa et al., 2011; Torrella et al., 2011). Table 1 shows the studies of the trans-critical CO_2 system with IHX.

Table 1. Studies of the transcritical CO_2 System with IHX.

Sl. no.	*Application*	*Focus*	*Improvement/Remarks*	*References*
1	Water heating	Effect of length of the tube of IHX on the overall performance	COP of the system improved for a certain discharge pressure	(Goo et al., 2005)
2	Air conditioning	Variable speed of cycle with EEV opening	The optimum compressor discharge pressure of the system reduced from 9.2 to 8.7 MPa	(Cho et al., 2007)
3	Air conditioning	Effect on the overall performance with/without IHX	Using the IHX, the COP was 10% better	(Aprea and Maiorino, 2008)
4	Air conditioning	Effect on the overall performance with/without IHX	An increment of the efficiency of the plant up to 12%	(Rigola et al., 2010)
5	Air conditioning	Effect of length of the tube of IHX on the overall performance	IHX provided a maximum COP improvement of up to 27%	(Nakagawa et al., 2011)
6	Freezing (up to -25 °C)	Effect on the overall performance with/without IHX	The IHX enhanced the exergy efficiency	(Shariatzadeh et al., 2016)
7	Air conditioning	Temperature and mass flow at the inlet boundary of both hot and cold streams	The high inlet temperature allowed the internal heat exchanger to be more efficient	(Ituna-Yudonago et al., 2017)
8	Air conditioning	The optimal control of gas cooler pressure with IHX by developing a control strategy	If capacity and appropriate overall heat transfer coefficient for gas cooler are achievable, the introduced concept can be effectively used as an analytical control method with reasonably good accuracy	(Kim et al., 2017)

1.1. Study objectives

This is the accepted version of an article published in Thermal Science and Engieering Progress
http://dx.doi.org/10.1016/j.tsep.2020.100590

Experimental evaluation of a 33kW cooling capacity multiejector based CO_2 cooling system in a series configuration will be carried out for a supermarket application at high ambient temperature conditions (up to 46^{o}C). Combination of HERE and LERE in series configuration to enhance the ejector pressure lift will be computed. Moreover, an additional improvement with the support of IHX in the system configuration will be projected. Zero superheat phenomena or flooding condition for evaporator will be examined. Improvements in performance of the system will be assessed in terms of COP, PIR and superheat reduction. Moreover, a comparative study will show the reported field results and tested system. The study will also determine the design operating conditions that must be maintained to ensure highest efficiently of CO_2 cooling system for the supermarket application at high ambient conditions.

1.2. Test-rig location and ambient conditions

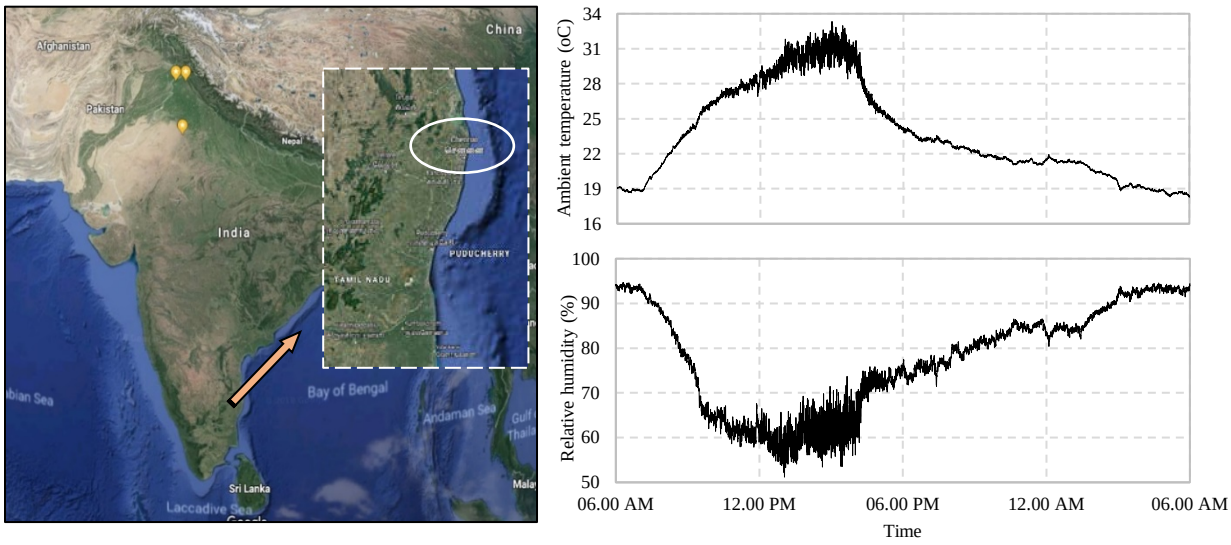

Figure 2. Location of CO_2 cooling test-rig for supermarket application and ambient conditions during the experimental evaluation.

Figure 2 shows the location of CO_2 cooling test-rig for supermarket application and ambient conditions during the experimental evaluation. The test-rig is installed in the southern Asia partition (Chennai, India) where the average ambient temperature conditions are quite high. The test-rig is operated, and the performance is evaluated for a typical day of summer 24th May 2019.

2. CO_2 test-rig description

This is the accepted version of an article published in Thermal Science and Engieering Progress
http://dx.doi.org/10.1016/j.tsep.2020.100590

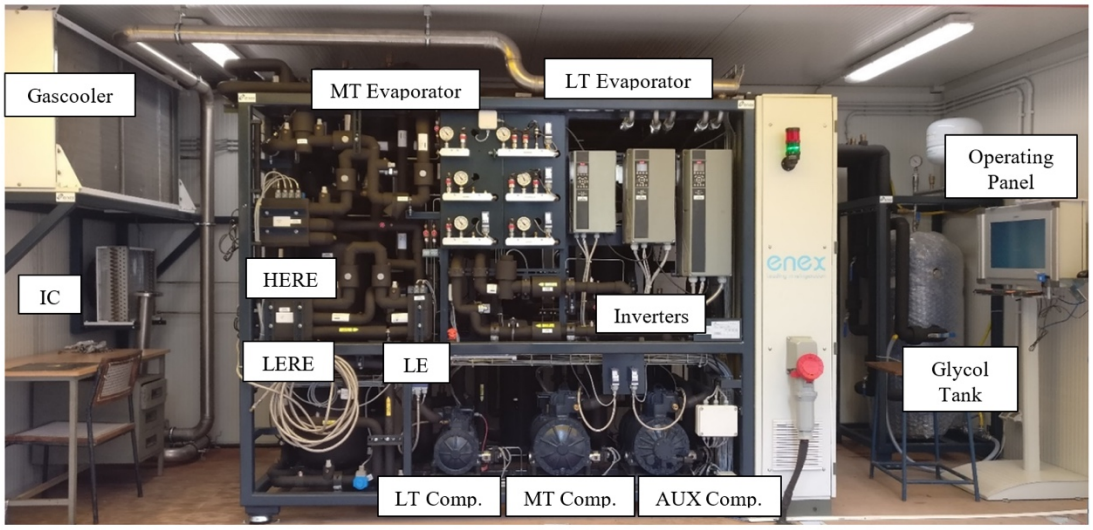

Figure 3. Picture of CO_2 cooling system test-rig.

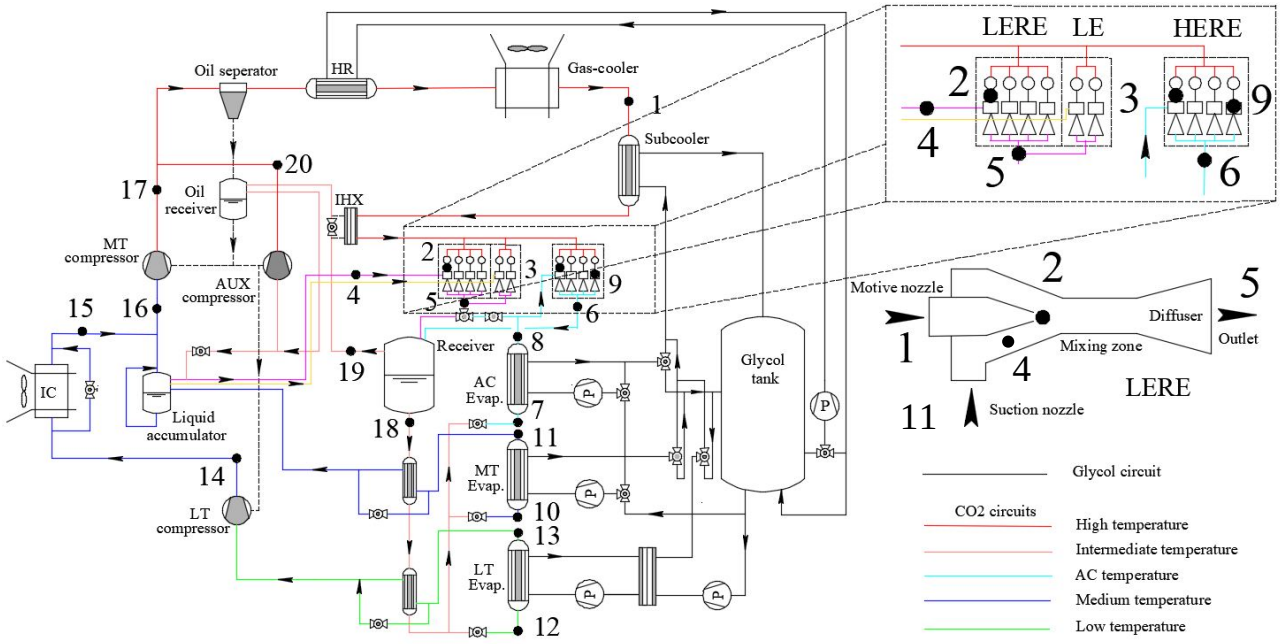

Figure 4. Schematic of CO_2 cooling system test-rig.

Figure 3 shows the picture of CO_2 cooling system test-rig and Figure 4 shows the schematic of CO_2 cooling system test-rig. The various pressure levels in the system are highlighted with the different colors. Compressor oil collection point in the CO_2 loop is also presented. The rig is fully instrumented and designed with a cooling capacity of 33 kW for supermarket cooling application to maintain three different evaporation temperature levels: -28°C for freezing, -6°C for refrigeration and +6°C for air conditioning. The test facility is equipped with a heat reclaim (water-

This is the accepted version of an article published in Thermal Science and Engieering Progress
http://dx.doi.org/10.1016/j.tsep.2020.100590

glycol solution), which is used to generate heat load towards the three evaporators from the water-cooled gas cooler in a closed loop with a glycol reservoir tank. Two water-glycol loop circuits are arranged with different glycol concentrations according to the cooling application (MT and LT).

Load of medium temperature (MT) and low temperature (LT) evaporators on secondary loop are operated by manually controlled EEVs. The temperature of LT and MT is controlled by compressor suction. The temperature level of the AC evaporator is controlled by the receiver pressure. Three compressors are arranged, LT and MT compressors and an additional AUX (AC) compressor is installed to handle high amounts of flash gas from the receiver which also enables so-called parallel compression. Three separate inverters are installed to control the compressor motor frequency to achieve the individual set-points. Two multiejectors are installed: one with a low ejection ratio (LERE) and other with a high ejection ratio (HERE). Each ejector has six slots or cartages to control the load variation in the system.

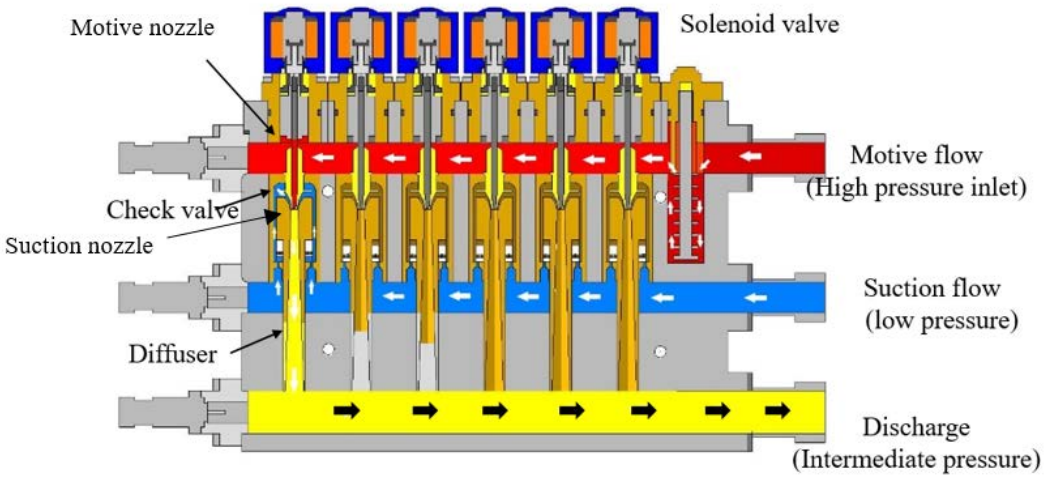

Figure 5. Internal structure of a two-phase multiejector.

Figure 5 shows the internal structure of a two-phase multi-ejector that is used in the CO_2 cooling supermarket test-rig. Significant function of the various internal parts of the multi-phase ejector are; the solenoid framed on the top, regulates the opening and closing of the solenoid valve of the cartage according to the capacity of the test-rig requested by the opening degree of the high-pressure expansion valve of the system. As the magnet energizes in the solenoid controller, the respective cartage needle lifts results in the valve opening, which further allows the high-pressure refrigerant to enter through the motive nozzle of the ejector. Due to which, low pressure is

This is the accepted version of an article published in Thermal Science and Engieering Progress
http://dx.doi.org/10.1016/j.tsep.2020.100590

generated at the suction nozzle, which results in the lifting of the check valve of the suction nozzle, which allows the fluid to enter the mixing chamber. Both motive and suction fluids blends in the mixing section of the ejector and high kinetic energy is formed in the motive stream before mixing. The mixture enters the diffuser section and the high kinetic energy is converted into pressure energy and the pressure increases to intermediate or discharge pressure which is more than the suction pressure. The different between these two is known as ejector pressure lift.

A liquid suction accumulator is also installed in order to enable a secure separation of liquid and vapor upstream of the compressors to allow a liquid over feed operation or flooding operation of the evaporators throughout the year. Temperature sensors, pressure sensors and energy meters are installed at various pressure levels of the test-rig to measure and evaluate the performance of the system and examine the various parameter variations. The system facilitates both manual and automatic optimization of the gas cooler pressure level with respect to the gas cooler outlet temperature. The test-rig facility also has a manual operated controller for the RPM of the two gas cooler fans to maintain various airflow rates to manipulate or adjust the refrigerant exit temperature in the gas cooler. Details of the various sensors installed in the CO_2 test-rig are tabulated in Table 2 and CO_2 system components details are tabulated in Table 3.

Table 2. Various sensors installed in the CO_2 test-rig.

S. no.	Sensor	Company	Model	Type	Range	Accuracy (% of measure value)
1.	Temperature	Danfoss	AKS 21M	B	-50 to 200°C	0.4
2.	Pressure	Danfoss	AKS 2050	----	up to 150 bar	0.5
3.	Energy meter	ISOIL	PT 500	IFX-M	3.0 $m^3 h^{-1}$	0.5
4.	Power meter	Danfoss	VFD	----	35-60 Hz	0.8

Table 3. CO_2 system components details.

Component	*Details*	*Units*	*Value /Type*
Gas cooler	Cooling medium		Air
	Coil rows		4
	Distribution circuits		8
	Fans		2
	Fin material		Aluminum
	Fin thickness	mm	0.3

This is the accepted version of an article published in Thermal Science and Engieering Progress
http://dx.doi.org/10.1016/j.tsep.2020.100590

	Fin spacing	mm	2.1
	Heat exchanger type		Fin-tube
	Maximum working pressure	bar	130
	Maximum operating temperature	°C	150
	Overall dimensions	mm	1895*471*832
	Pipe material		Copper
	Rated capacity	kW	54
LT Compressor	Bore/stroke	mm	22/22
	Displacement	$m^3 h^{-1}$	1.46
	Design		Reciprocating
	Model		Dorin CD 300H
	No of cylinders		2
MT Compressor	Bore/stroke	mm	34/27.5
	Displacement	$m^3 h^{-1}$	4.34
	Design		Reciprocating
	Model		Dorin CH 700H
	No of cylinders		2
AUX Compressor	Bore/stroke	mm	42/37
	Displacement	$m^3 h^{-1}$	10.70
	Design		Reciprocating
	Model		Dorin CD 1300H
	No of cylinders		2
Oil	Compressors oil		PAG 68, Daphne hermetic oil
LT Evaporator	Design		Shell and tube exchanger
	Heat exchanger length	mm	3120
	Rated capacity	kW	3
	Shell material		Steel
	Shell outer diameter	mm	60.3
	Suction tube outer diameter	mm	11
	Tube material		Copper
MT Evaporator	Design		Shell and tube exchanger
	Heat exchanger length	mm	1980
	Rated capacity	kW	10
	Shell material		Steel
	Shell outer diameter	mm	68
	Suction tube outer diameter	mm	14
	Tube material		Copper

This is the accepted version of an article published in Thermal Science and Engieering Progress
http://dx.doi.org/10.1016/j.tsep.2020.100590

AC Evaporator	Design		Shell and tube exchanger
	Heat exchanger length	mm	1734
	Rated capacity	kW	20
	Shell material		Steel
	Shell outer diameter	mm	76
	Suction tube outer diameter	mm	16
	Tube material		Copper
Heat recovery	Design		Shell and tube exchanger
	Heat exchanger length	mm	2120
	Rated capacity	kW	33
	Shell material		Steel
	Shell outer diameter	mm	89
	Suction tube outer diameter	mm	11
	Tube material		Copper

3. CO_2 cooling system for supermarket operational mode

3.1. Multiejector operation in a series configuration

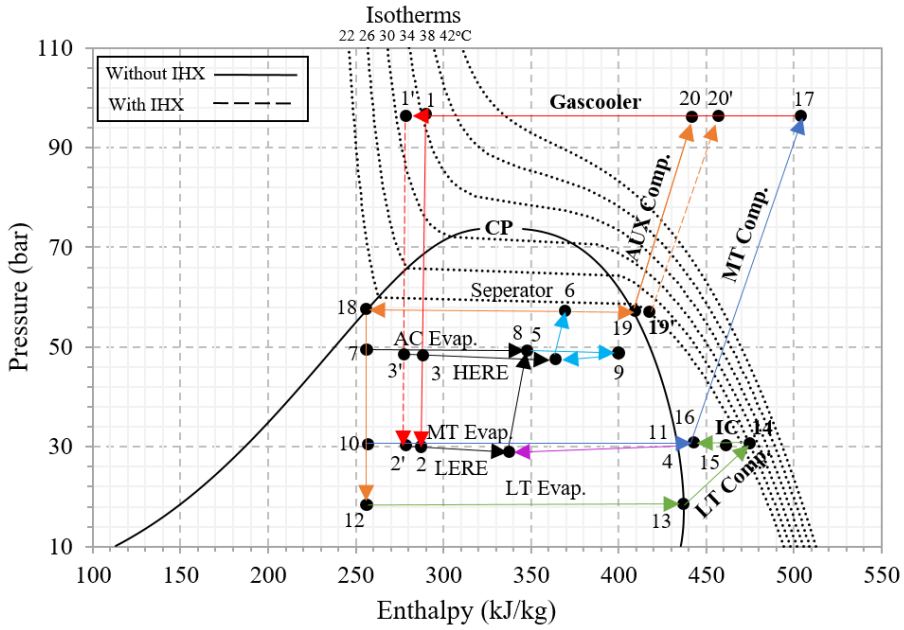

Figure 6(a). Ph plot of the test-rig's supermarket cooling operational module for an Indian supermarket.

This is the accepted version of an article published in Thermal Science and Engieering Progress
http://dx.doi.org/10.1016/j.tsep.2020.100590

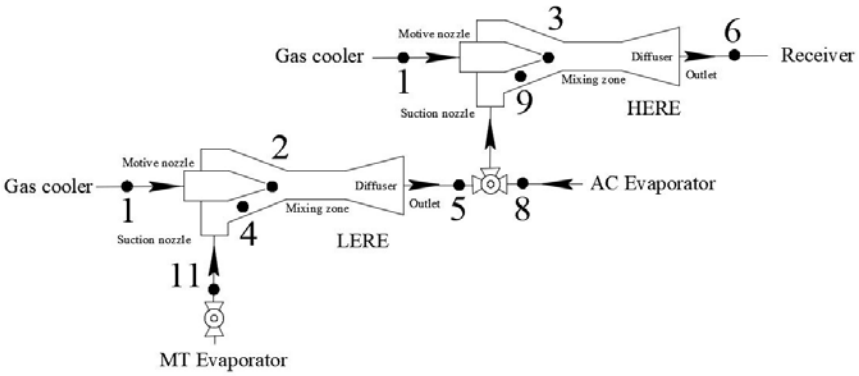

Figure 6(b). Series operation of two-phase ejectors (LERE and HERE) in the supermarket cooling operational module for an Indian supermarket.

Figure 6(a) shows the Ph plot of the test-rig's supermarket cooling operational module for an Indian supermarket and Figure 6(b) shows the series operation of two-phase ejectors (LERE and HERE) in the supermarket cooling operational module for an Indian supermarket. CO_2 gas from the air cooled gascooler (state 1) at high pressure and high temperature is divided into two motive fluid streams for the two-phase multiejectors; LERE (state 2) and HERE (state 3). The suction fluid stream of the LERE (state 4) is the combination of MT evaporator (state 11) and vapor from the liquid accumulator. With the support of LERE, the fluid pressure increases up to the AC evaporator pressure level (state 5), which eventually unloads the MT compressor load. Similarly, the suction fluid of the HERE is the combination of the AC evaporator (state 8) and LERE's intermediate fluid (state 9). Further, the combination of fluid and high pressure and high temperature CO_2 gas from the air cooled gascooler (state 3), forms high kinetic energy before the mixing section of the HERE and the pressure of the fluid increases by converting kinetic energy into pressure energy in the diffuser. As a result, the pressure of the fluid increases from the AC evaporator to the receiver pressure level or separator (state 6). Further, the vapor (state 20) and liquid (state 19) get separated in the receiver tank. The fluid (state 19) is directed towards the three evaporators; AC (state 7), MT (state 10) and LT (state 12) after throttling the liquids to the corresponding evaporator pressures through the feeding valves. The LT evaporator exit fluid (state 13) is compressed separately up to the suction pressure level of the MT evaporator with the support of LT compressor. Pure vapor (state 11) from the MT suction accumulator is further mixed with the discharge of the LT compressor (state 14) after passing through the intercooler (IC) (state 15). Fluid (state 16) is compressed by the MT compressor up to the gascooler pressure (state 17). The

This is the accepted version of an article published in Thermal Science and Engieering Progress
http://dx.doi.org/10.1016/j.tsep.2020.100590

combination of the compressed vapor through the MT compressor (state 17) and AUX compressor (state 20), passes through the water cooled and air cooled gascooler. Moreover, the IHX is incorporated in the test-rig to improve the performance of the CO_2 supermarket configuration and projected as state (1' to 2' and 19' to 20', depicted the respected processes in the cycle.

3.2. Evaporator flooding/non-flooding conditions

In order to improve the heat transfer characteristics of the evaporators and overall performance of the CO_2 cooling system, flooding of the evaporator is also reported as one of the prominent approach (Minetto et al., 2014).

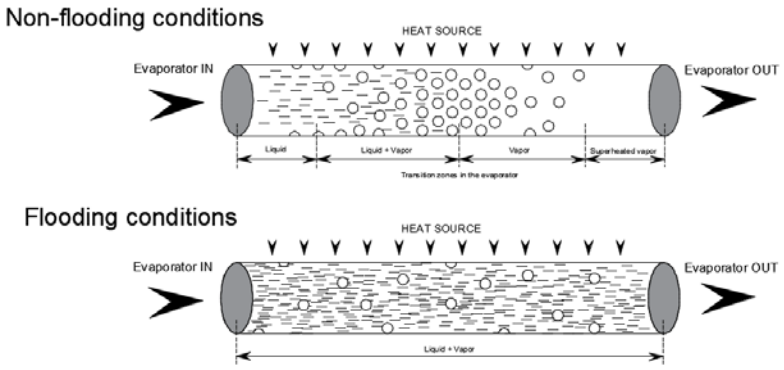

Figure 7. Flooding/non-flooding during ideal conditions of the evaporator.

Figure 7 shows the flooding/non-flooding during ideal conditions of the evaporator. Aiming to the ideal conditions for the evaporator, during non-flooding conditions, the single-phase fluid (liquid) enters and leaves as a superheated vapor. However, during evaporator flooding conditions, single-phase (liquid) enters, but, leaves as a two-phase fluid (liquid and vapor). The overfeeding of the liquid refrigerant provides complete wetness to the inner surface of the evaporator and this result in overall improvement of its heat transfer characteristics.

Figure 8 shows the system components involved during the evaporator flooding in the test-rig. The motive nozzle of the liquid ejector is connected to the gas cooler discharge and the motive nozzle with liquid suction accumulator. A multi-slot liquid ejector is employed in the system configuration to overfeed or flood the MT evaporator. Two-slot liquid ejector is operated in such a way that it maintains the CO_2 system capacity and provide enough refrigerant to flood the MT evaporator. Therefore, the extra refrigerant is drawn from the liquid suction accumulator. To

This is the accepted version of an article published in Thermal Science and Engieering Progress
http://dx.doi.org/10.1016/j.tsep.2020.100590

overfeed or flood the MT evaporator, the excess CO2 liquid is sent to the receiver from liquid suction accumulator by controlling the two-slot liquid ejector openings manually. Moreover, the percentage opening degree (OD) of the expansion valve (EV) of the MT evaporator is controlled by the system service tool to a maximum level. It is observed that, during the operation, superheat at the exit of the evaporator provides clear indication of the evaporator under flooding or non-flooding conditions. Zero or minimum superheat at the outlet of the evaporator is maintained by simultaneous controlling of both OD of the expansion valve and two liquid ejector slot openings.

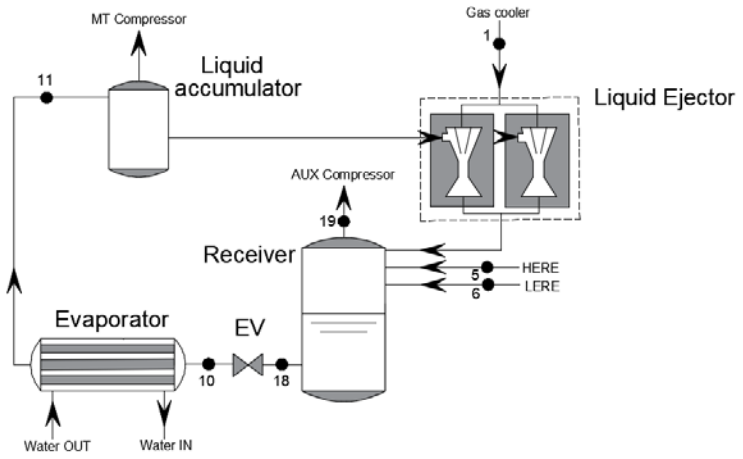

Figure 8. System components involved during the evaporator flooding in the test-rig.

4. Performance evaluation and experimental data reduction

The installed test-rig has the service tool designed by M/s Danfoss. The service tool has full control of all components of the CO_2 cooling system and secondary circulation sides projected in Figure 5. During the test, first, the CO_2 loop parameters such as temperature of the three evaporators (MT, LT and AC), receiver pressure (RP) and gas cooler outlet temperature are determined. The gas cooler pressure is automatically optimized according to the gas cooler outlet temperature with the controlling sensor provided by Danfoss in the system. After logging the CO_2 side operating parameters in the service tool, the load of three evaporators (MT, LT and AC) are monitored. The load on the evaporator is adjusted after 30 minutes to maintain it constant by the secondary glycol loop. The loads of the three evaporators are controlled by changing the mass flow rate of the glycol solution in the secondary loop. It is observed that the system requires approximately 2 hours to reach steady state. A steady state of the system is considered with constant thermal loads on the evaporators, constant evaporator temperature conditions, constant gas cooler outlet temperature

This is the accepted version of an article published in Thermal Science and Engieering Progress
http://dx.doi.org/10.1016/j.tsep.2020.100590

and receiver pressure. The CO_2 system performance is evaluated for only steady state conditions averaged hourly data for a gas cooler outlet temperature. The averaged output values of the various parameters are further used for the performance evaluation of the CO_2 system. Properties of CO_2 and water/glycol solution are obtained with the support of REFPROP 9.0 and the various system operating parameters used for performance evaluation are tabulated in Table 4.

Table 4. Various system operating parameters used for performance evaluation.

Operating Parameter	**Units**	**Value/Range**
Gas cooler outlet temperature	°C	36 to 46
Gas cooler pressure	bar	80 to 115
Receiver pressure	bar	45 to 46
AC evaporator temperature	°C	+6
MT evaporator temperature	°C	-6
LT evaporator temperature	°C	-28

The performance of the ejector based CO_2 cooling system for supermarket applications at high ambient temperature is computed using the following equations.

- Coefficient of Performance *(COP)* of the CO_2 cooling system is computed by,

$$COP = \frac{Q_{AC}+Q_{MT}+Q_{LT}}{P_{AUX,}+P_{MT}+P_{LT}} \quad (1)$$

Where, load on the three evaporators AC, MT and LT of the system is computed from the glycol side by,

$$\dot{Q}_{AC} = \dot{m}_{AC} * c_p * (T_{AC\_o} - T_{AC\_i}) \quad (2)$$

$$\dot{Q}_{MT} = \dot{m}_{MT} * c_p * (T_{MT\_o} - T_{MT\_i}) \quad (3)$$

$$\dot{Q}_{LT} = \dot{m}_{LT} * c_p * (T_{LT\_o} - T_{LT\_i}) \quad (4)$$

- Pressure lift (*PL*) generated by the two-phase HERE is computed as,

$$PL = P_6 - P_3 \quad (5)$$

- Power Input Ratio (*PIR*): a simplified method based on measurement of power input and the comparison of the minimum ideal required power in the Carnot cycle is used (Figure 9). Power Input Ratio (PIR) can be calculated for any ambient temperature and reference temperature levels such as utilities at LT, MT, AC, heating, and domestic hot water ,(Banasiak et al., 2019).

This is the accepted version of an article published in Thermal Science and Engieering Progress
http://dx.doi.org/10.1016/j.tsep.2020.100590

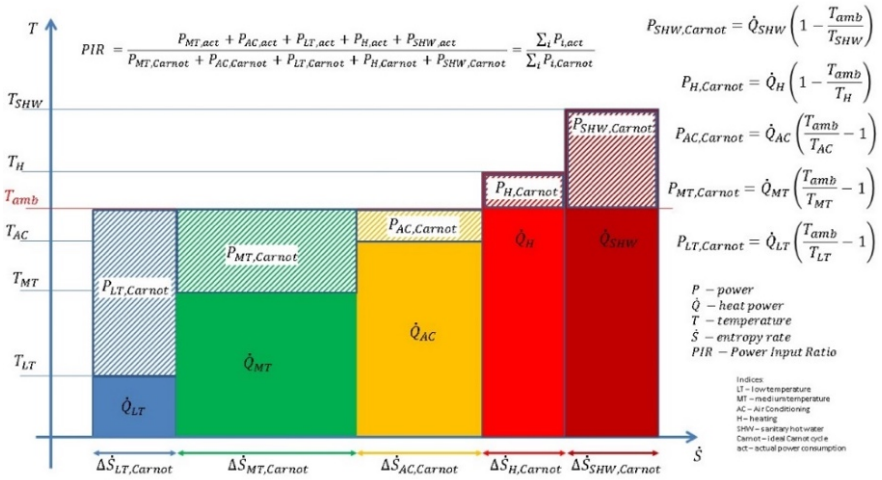

Figure 9: Power input and the comparison of the minimum ideal required power in the Carnot cycle.

$$PIR = \frac{P_{AUX}+P_{MT}+P_{LT}}{P_{AUX,Car}+P_{MT,Car}+P_{LT,Car}} \quad (6)$$

where, Carnot power consumption of the three compressors AUX, MT and LT is computed by,

$$P_{AUX,Car} = \frac{\dot{Q}_{AC}}{T_{UT\_AC}} * (T_{amb} - T_{UT\_AC}) \quad (7)$$

$$P_{MT,Car} = \frac{\dot{Q}_{MT}}{T_{UT\_MT}} * (T_{amb} - T_{UT\_MT}) \quad (8)$$

$$P_{LT,Car} = \frac{\dot{Q}_{LT}}{T_{UT\_LT}} * (T_{amb} - T_{UT\_LT}) \quad (9)$$

The utility temperatures (T_{UT}) or product temperature assumed for the three evaporators AC, MT and LT are 22°C, 4°C and -18°C, respectively.

4.1. Uncertainty analysis

In the present experimental study, Type B evaluation of the standard uncertainty is adopted as suggested (Taylor and Kuyatt, 2001), which is based on scientific judgement from the information available during measurements of the various parameters. Therefore, the higher and lower limits of the measured quantity from the sensors and uncertainty in the direct measurement is computed using Eq. (10). Combined standard uncertainty of the measured value is estimated using the estimated standard derivation of the results and the uncertainty of the measured quantity and

This is the accepted version of an article published in Thermal Science and Engieering Progress
http://dx.doi.org/10.1016/j.tsep.2020.100590

computed using Eq. (11). Uncertainty in direct measurements by the temperature sensor, pressure sensor and energy meter are 0.69%, 0.119% and 0.093% respectively.

$$x_i = \frac{Accuracy\ of\ the\ measured\ value}{\sqrt{3}} \tag{10}$$

$$u_c{}^2(y) = \sum_{i=1}^{N} \left(\frac{\partial f}{\partial x_i}\right)^2 u^2(x_i) \tag{11}$$

5. Results and discussion

5.1. Variation of the gas cooler pressure

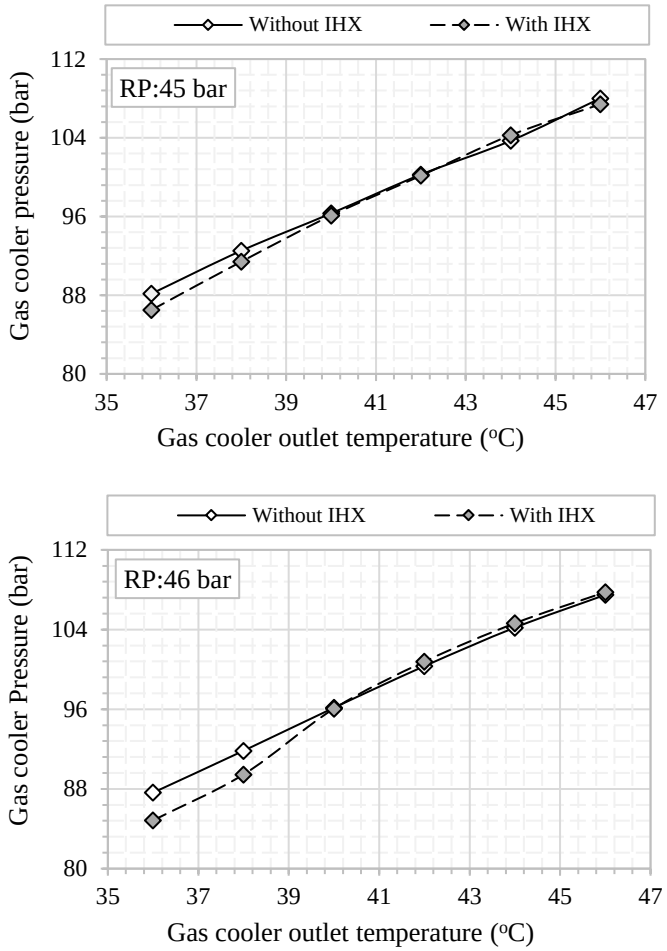

Figure 10. Gas cooler pressure with gas cooler outlet temperature at various receiver pressure with/without IHX.

The gas cooler pressure in the test-rig is optimized and controlled by the Danfoss controllers installed to obtain the optimum COP of the system. The controller installed in the

This is the accepted version of an article published in Thermal Science and Engieering Progress
http://dx.doi.org/10.1016/j.tsep.2020.100590

system follows the S-shape isotherm curve along with a control strategy to obtain the optimum point of gas cooler pressure for every gas cooler outlet temperature. The performance of the CO_2 test-rig is evaluated for the two receiver pressures 45 bar and 46 bar. Figure 10 shows the gas cooler pressure with gas cooler outlet temperature at various receiver pressure with/without IHX. Three evaporator temperatures are kept constant (LT: -28°C MT: -6°C and AC: +6°C). It is observed that as the gas cooler outlet temperature increases, the gas cooler pressure also increases, following the S-shape isotherms. But it is also observed that the gas cooler pressure obtained for the lower gas cooler outlet temperatures, such as 36°C and 38°C, is comparatively less in the case of the CO_2 system with IHX. However, for the higher gas cooler outlet temperature more than 38°C, the gas cooler pressure of the system for both with/without IHX is almost same. A similar trend is observed during the 46 bar receiver pressure as well. Figure 10 also projects that the system with IHX is performing better at lower gas cooler outlet temperature by consuming less power by the MT and AUX compressors to obtain the higher gas cooler pressure as compare to the system without IHX. Moreover, the margin is relatively more for 46 bar receiver pressure in the system with/without IHX. Hence projecting 46 bar receiver pressure as the optimum intermediate pressure.

5.2. Variation of the compressors discharge temperature

Figure 11 shows the compressor discharge temperature with the gas cooler outlet temperature at various receiver pressure with/without IHX. The discharge temperature of three compressor are projected for 45 bar and 46 bar receiver pressures by keeping three evaporators temperature constant LT: -28°C MT: -6°C and AC: +6°C. Therefore, the suction temperatures of the LT and MT are also constant. It is observed that the discharge temperature of the MT and LT compressors are almost same for the both receiver pressures 45 and 46 bar for the CO_2 cooling system with/without IHX. It is due to the fact that the effect of IHX is completely isolated from the MT loop and LT of the CO_2 cooling system. However, the discharge temperature of the AUX compressor is increasing for the CO_2 cooling system with IHX for the both receiver pressures. The additional enhancement in the discharge temperature of the AUX compressor is due to the coupling of IHX with the suction of the AUX compressor. Furthermore, it is also observed that the discharge temperature of the MT compressor is comparatively lower for the 46 bar receiver pressure as compare to the 45 bar receiver pressure.

This is the accepted version of an article published in Thermal Science and Engieering Progress
http://dx.doi.org/10.1016/j.tsep.2020.100590

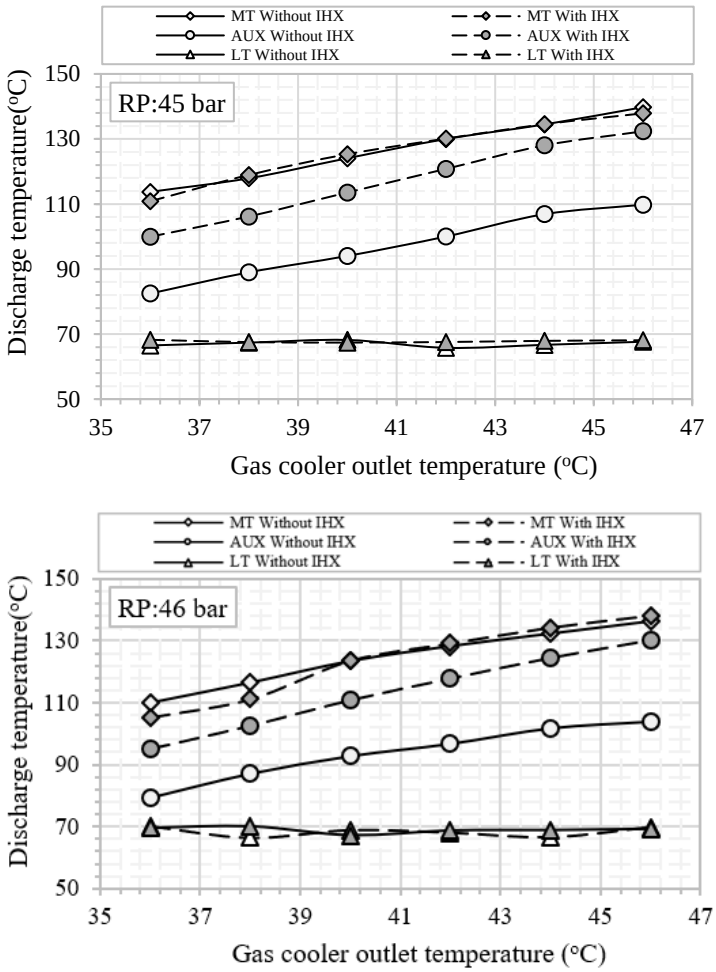

Figure 11. Compressors discharge temperature with gas cooler outlet temperature at various receiver pressure with/without IHX.

5.3. Variation of the pressure lift

Figure 12 shows the ejector pressure lift with gas cooler outlet temperature at various receiver pressures with/without IHX. The pressure lift in the CO_2 cooling system is computed as the difference between receiver pressure and AC evaporator pressure, and the same is computed using Eq. (5). It is observed that the pressure lift by the ejector increases with respect to the gas cooler outlet temperature increases. It is due to the fact that as the gas cooler outlet temperature increases, the gas cooler pressure or the motive nozzle pressure also increases. Very marginal improvement in the pressure lift is observed with respect to the IHX in the system configuration. Moreover, it is also observed that the pressure lift at 46 bar receiver pressure of the CO_2 cooling system is higher

This is the accepted version of an article published in Thermal Science and Engieering Progress
http://dx.doi.org/10.1016/j.tsep.2020.100590

as compare to the 45 bar receiver pressure. The enhancement in motive nozzle mass flow rate at 46 bar receiver pressure could be the reason for the same. The maximum pressure lift observed from the CO_2 cooling system is approximately 5.5 bar for 46 bar receiver pressure.

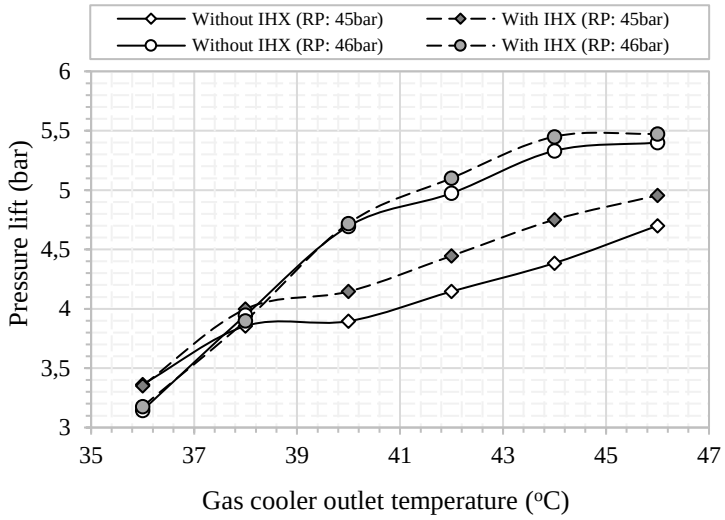

Figure 12. Ejector pressure lift with gas cooler outlet temperature at various receiver pressures with/without IHX.

5.4. Variation of the coefficient of performance (COP)

COP is one of the important performance parameter and the same is computed using Eq. (1). The system performance evaluation is carried out at constant LT: -28°C MT: -6°C and AC: +6°C evaporator temperatures. Figure 13 shows the COP of the CO_2 cooling system with gas cooler outlet temperature at various receiver pressures with/without IHX. It is observed that as the gas cooler outlet temperature increases, the system COP decreases. It is ascribed to the fact that as the gas cooler outlet temperature increases, the input power required to provide the optimum gas cooler pressure by the MT and AUX compressors also increases. A similar behavior is observed for the both receiver pressure with/without IHX. However, the discharge temperature of the gas cooler is comparatively less in the system with IHX, which further results in higher COP of the CO_2 system. The reason behind the same is due to the reduction in the MT and AUX compressor discharge pressure with the support of IHX in the system configuration. Moreover, it is also observed that the COP of the CO_2 system with 46 bar receier pressure is comparatively higher than the system with 45 bar receiver pressure. The lower discharge temperature of MT and AUX compressors at 46 bar receiver pressure is the reason which is also projected with the support of Figure 11. The maximum COP of the CO_2 cooling system with IHX observed is in the range 1.8

This is the accepted version of an article published in Thermal Science and Engieering Progress
http://dx.doi.org/10.1016/j.tsep.2020.100590

to 2.75 for 46 bar receiver pressure which is approximately 7.2% enhancement in the COP as compare to the system without IHX.

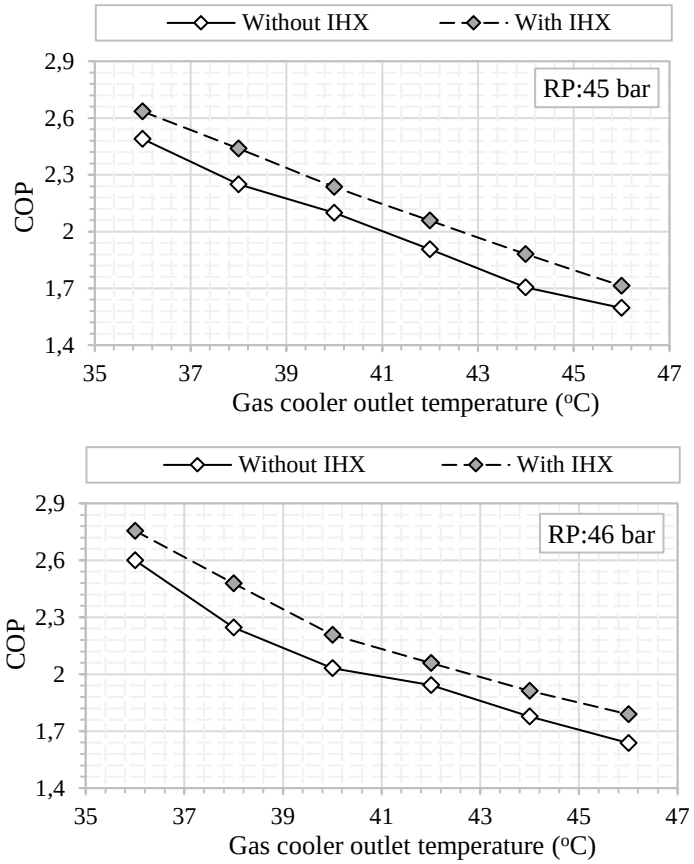

Figure 13. COP of the CO_2 cooling system with gas cooler outlet temperature at various receiver pressure with/without IHX.

5.5. Variation of the power input ratio (PIR)

Figure 14 shows PIR of the CO_2 cooling system with gas cooler outlet temperature at various receiver pressure with/without IHX. PIR of the CO_2 cooling system with/without IHX, and the same is computed using Eq. (6). It is observed that as the gas cooler outlet temperature increases the PIR of the system increases. It is ascribed to the fact that as the gas cooler pressure corresponding to the gas cooler outlet temperature increases, higher pressure lift from the compressors are requested by the system. As a result power input to the MT and AUX compressors increases, which results in higher PIR. However, it is observed that the PIR for the system with IHX is significantly less than the system without IHX. The maximum PIR of the CO_2 cooling system with IHX is in the range 4.7 to 5 for 46 bar receiver pressure which is approximately 6.2%

This is the accepted version of an article published in Thermal Science and Engieering Progress
http://dx.doi.org/10.1016/j.tsep.2020.100590

reduction on average in the PIR of the CO_2 cooling system. Moreover, it is also observed that the system PIR for the 46 bar receiver pressure is comparatively less than 45 bar receiver pressure.

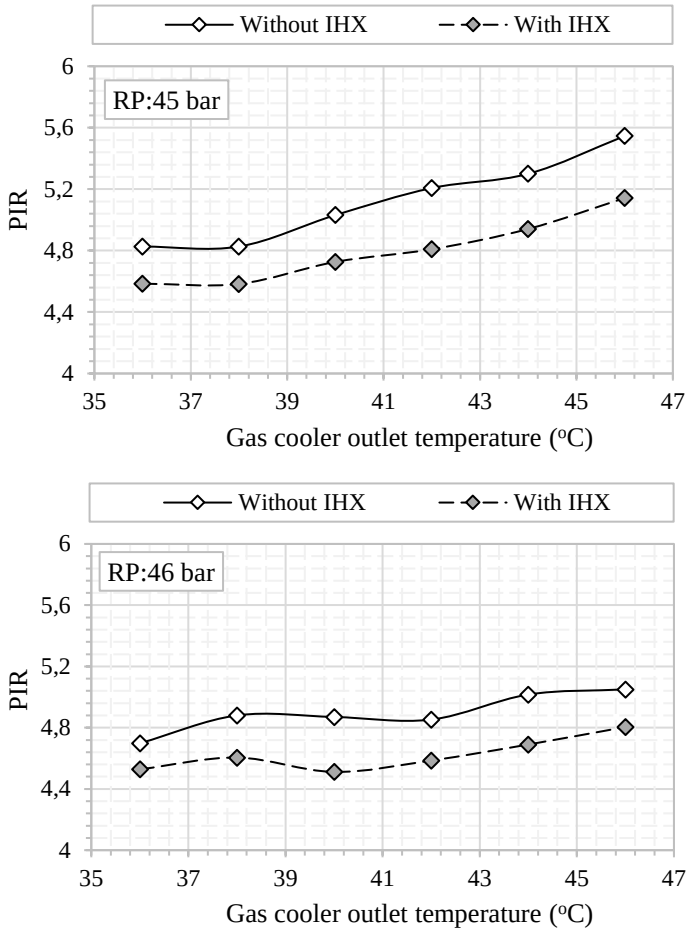

Figure 14. PIR of the CO_2 cooling system with gas cooler outlet temperature at various receiver pressure with/without IHX.

5.6. Variation of the evaporator superheat

During the operation, the flooding/non-flooding conditions are confirmed with the support of side glasses installed at the evaporator outlet. Figure 15 shows a visual side glass at the outlet of the evaporator during non-flooding/flooding conditions. During the operation, the overfeeding and flooded operation of the evaporator is confirmed visually by the side glass at the outlet of the evaporator. It is observed that, during the non/flooding condition or superheated condition, only single phase (vapor) can be observed at the outlet of the evaporator, but during the evaporator flooding condition, two-phase (liquid and vapor) is observed at the outlet of the evaporator.

This is the accepted version of an article published in Thermal Science and Engieering Progress
http://dx.doi.org/10.1016/j.tsep.2020.100590

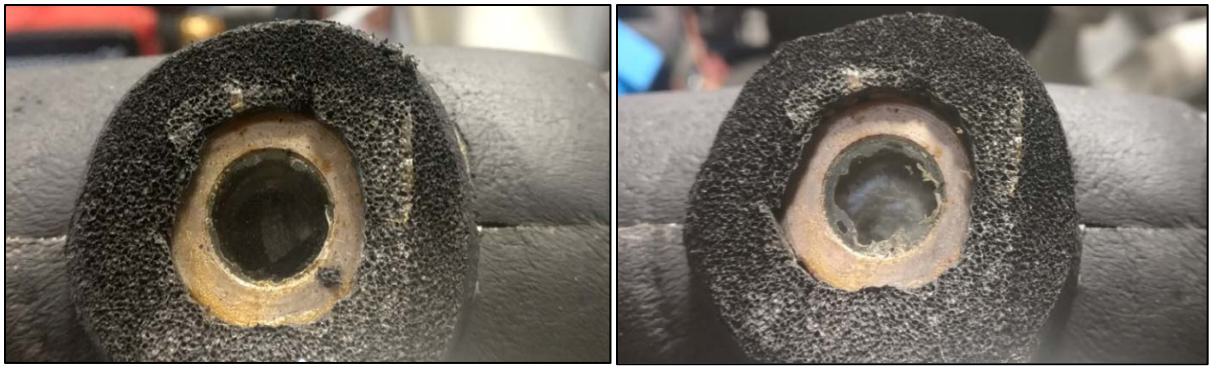

Figure 15. Visual side glass at the outlet of the evaporator during non-flooding/flooding conditions.

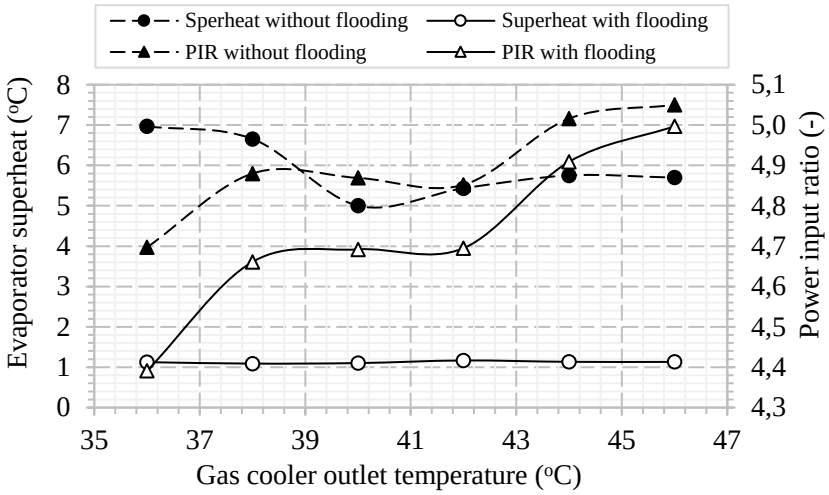

Figure 16. Evaporator superheat and PIR during flooding/non-flooding conditions.

Figure 16 shows the evaporator superheat and PIR during flooding/non-flooding conditions. During the non-flooding conditions, the maximum superheat observed at the outlet of the evaporator is 7K. However, during the flooding conditions, the maximum superheat observed at the evaporator outlet is 1K at various gas cooler outlet temperature. However, the reason behind 1K superheat at the outlet of the evaporator is the fixing position of the temperature sensors which are basically installed on the outer surface of the evaporator coil in the system. Therefore, it is confirmed that the sensor is recording the average surface temperature at the outlet of the MT evaporator. Furthermore, PIR of the CO_2 system is increasing as the gas cooler outlet temperature increasing. This is ascribed to the increasing input power to the compressor to attain the requested pressure lift by the compressor with respect to the gas cooler outlet temperature or gas cooler

This is the accepted version of an article published in Thermal Science and Engieering Progress
http://dx.doi.org/10.1016/j.tsep.2020.100590

pressure. However, during the flooding conditions, it is observed that the system PIR is reducing. This is due to the reduction in the pressure ratio of the compressor required to attain the same gas cooler pressure level, which therefore reduces the power input to the compressor.

Figure 17 shows the reduction in evaporator superheat and PIR during flooding condition. It is observed that the maximum percentage reduction in the MT evaporator superheat and PIR of the CO_2 cooling system is approximately 83.84% and 6.51% respectively during flooding conditions. Therefore, projecting evaporator flooding as a potential improvement in the system configuration to enhance the overall performance of the CO_2 cooling system for supermarket application at high ambient temperature conditions.

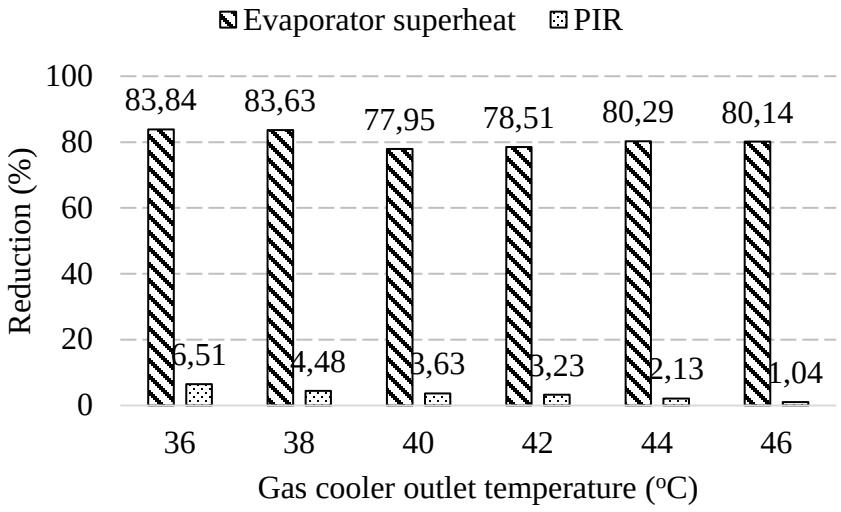

Figure 17. Reduction in evaporator superheat and PIR during flooding condition.

6. Comparative analysis

Figure 18 shows the comparison between COP of the five CO_2 supermarkets (field data) and proposed CO_2 cooling system for supermarket. The experimental result obtained from the present CO_2 cooling system test-rig for supermarket application is compared with the field test results obtained from the five different CO_2 supermarkets in Sweden (Sawalha and Karampour, 2015). All supermarkets are employed to maintain two different medium and low temperature levels. The maximum ambient temperature for which the performance of the five supermarkets reported is 31.2°C but the present study is reported for 46°C. A similar trend is observed from the present study as compare to the field data results i.e. COP is reducing with respect to the ambient

This is the accepted version of an article published in Thermal Science and Engieering Progress
http://dx.doi.org/10.1016/j.tsep.2020.100590

temperature. The COP of the present system is low as compared to the reported field results. Which is obvious due to high throttling losses in the CO_2 cycle while operating at high gas cooler pressure and gas cooler outlet temperature. It is observed that the COP of the present system configuration tested at high ambient temperature is acceptable for high ambient temperature conditions during the comparative analysis. The maximum COP of the present CO_2 cooling system is equal to the COP of the three CO_2 cooling supermarkets reported at low ambient temperature conditions.

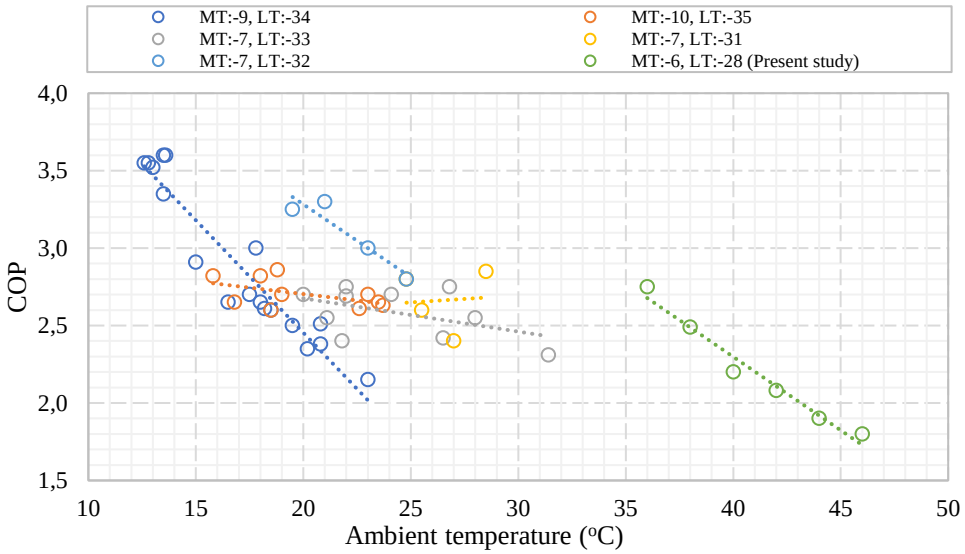

Figure 18. Comparison between the COP of the five CO_2 supermarkets (field data) and proposed CO_2 cooling system for supermarket.

7. Conclusions and scope

Performance evaluation of a novel multiejector CO_2 cooling system test-rig for Indian supermarket application is carried out in the present experimental study and its stability at high ambient temperature conditions. CO_2 cooling system configuration is tested with one low ejection ratio ejector (LERE) and one high ejection ratio ejector (HERE) equipped in a series configuration. The performance of the CO_2 cooling system is evaluated with constant evaporator temperatures LT: -28°C, MT: -6°C and AC: +6°C for 45 bar to 46 bar receiver pressure at various gas cooler outlet temperature upto 46°C. The performance of the CO_2 cooling system is evaluated in terms of pressure lift, coefficient of performance (COP), power input ratio (PIR) and evaporator superheat.

It is concluded that the proposed CO_2 cooling system with ejectors in series configuration is the effective option for the Indian supermarket cooling systems with its promising high COP and

This is the accepted version of an article published in Thermal Science and Engieering Progress
http://dx.doi.org/10.1016/j.tsep.2020.100590

stable operation at high ambient temperature conditions. During the testing it is observed that the CO_2 cooling system with/without IHX is operated successfully up to ~110 bar gas cooler pressure, for the typical Indian operating conditions with stable operation at 45 bar and 46 bar receiver pressure. Also, the pressure lift through the two-phase ejector is significant at high ambient temperature. Improvement in the CO_2 cooling system performance is also explored with the use of internal heat exchanger (IHX) in the system configuration.

It is observed that the CO_2 cooling system is performing better with 46 bar receiver pressue for various gas coole outlet temperature. Moreover, the improvement in the overall performance of the CO_2 cooling system with the support of IHX is also conceived as an opportunity at high ambient temperature conditions. Reduction in the PIR of the system due to lowering of compressor discharge temperature eventually results in reduced operating pressure of the gas cooler and which overall effects the COP enhancement. The maximum COP of the CO_2 cooling system with IHX observed is in the range 1.8 to 2.75 for 46 bar receiver pressure which is approximately 7.2% enhancement in the COP as compare to the system without IHX.

The impact of the liquid ejector to overfeed or flood the evaporator is experimentally tested as well. With the evaporator flooding, reduction in the superheat at the evaporator outlet to a significant level is observed, which results in a substantial reduction in the system PIR. Moreover, a significant reduction is observed in the PIR of the CO_2 cooling system with IHX in the system configuration and with evaporator flooding as 6.2% and 6.5% respectively. The results of the present experimental study proves the concept of ejectors in series configuration and flooding the evaporators as an opportunity for the Indian supermarket cooling systems at high ambient temperature conditions.

During the comparitive analysis between the present experimental study and the reported field data from the CO_2 supermarket cooling system, it is observed that the proposed CO_2 cooling system with series ejector configuration may perform more efficiently than the existing systems at low ambient temperature conditions. The future work will progress with different temperature levels of LT, MT and AC evaporator at ambient temperature conditions.

Acknowledgements

The research work presented is part of an ongoing Indo-Norwegian project “INDEE” funded by the Ministry of Foreign Affairs, Government of Norway, coordinated by SINTEF, Norway. The

Indian authors acknowledge the additional support received from the Department of Science and Technology (DST) under project: PDF/2017/000083.

Nomenclature

AC	Air conditioning	
AUX	Auxiliary compressor	
COP	Coefficient of Performance	
c_p	Specific heat	(kW kg^{-1} K^{-1})
EV	Expansion valve	
GWP	Global warming potential	
IHX	Internal heat exchanger	
LERE	Low ejection ratio ejector	
LT	Low temperature	
$\dot{m}$	Mass flow rate	(kg s^{-1})
MT	Medium temperature	
OD	Opening degree	
ODP	Ozone depletion potential	
P	Power consumption	(kW)
PIR	Power input ratio	
PL	Pressure lift	
$\dot{Q}$	Heat transfer rate	(kW)
RP	Receiver pressure	
CO_2	Carbon dioxide	
UT	Utility Temperature	

Subscript

amb	ambient
car	Carnot
i,o	inlet and outlet

References

Aprea, C., Maiorino, A., 2008. An experimental evaluation of the transcritical CO2 refrigerator

This is the accepted version of an article published in Thermal Science and Engieering Progress
http://dx.doi.org/10.1016/j.tsep.2020.100590

performances using an internal heat exchanger. Int J Refrig 31, 1006–1011. doi:10.1016/j.ijrefrig.2007.12.016

Banasiak, K., Hafner, A., 2013. Mathematical modelling of supersonic two-phase R744 flows through converging-diverging nozzles: The effects of phase transition models. Appl Therm Eng 51, 635–643. doi:10.1016/j.applthermaleng.2012.10.005

Banasiak, K., Hafner, A., Kriezi, E.E., Madsen, K.B., Birkelund, M., Fredslund, K., Olsson, R., 2015a. Development and performance mapping of a multi- ejector expansion work recovery pack for R744 vapour compression units. Int J Refrig 57, 265–276. doi:10.1016/j.ijrefrig.2015.05.016

Banasiak, K., Hafner, A., Kriezi, E.E., Madsen, K.B., Birkelund, M., Fredslund, K., Olsson, R., 2015b. Development and performance mapping of a multi- ejector expansion work recovery pack for R744 vapour compression units. Int J Refrig 57, 265–276. doi:10.1016/j.ijrefrig.2015.05.016

Banasiak, K., Singh, S., Hafner, A., Prakash, M.P., Neksa, P., Pardinas, A., 2019. Experimental investigation of CO2 systems for Indian supermarkets with parallel configuration of multiejectors (INDEE), in: International Congress. doi:10.18462/iir.icr.2019.797

Bhatkar, V.W., Kriplani, V.M., Awari, G.K., 2013. Alternative refrigerants in vapour compression refrigeration cycle for sustainable environment : a review of recent research 871–880. doi:10.1007/s13762-013-0202-7

Calm, J.M., 2002. Emissions and environmental impacts from air-conditioning and refrigeration systems. Int J Refrig 25, 293–305. doi:10.1016/S0140-7007(01)00067-6

Cho, H., Ryu, C., Kim, Y., 2007. Cooling performance of a variable speed CO2 cycle with an electronic expansion valve and internal heat exchanger. Int J Refrig 30, 664–671. doi:10.1016/j.ijrefrig.2006.10.004

Dai, Y., Wang, J., Gao, L., 2009. Exergy analysis, parametric analysis and optimization for a novel combined power and ejector refrigeration cycle. Appl Therm Eng 29, 1983–1990. doi:10.1016/j.applthermaleng.2008.09.016

Goo, S., Jo, Y., Lee, G., Soo, M., 2005. The performance of a transcritical CO2 cycle with an internal heat exchanger for hot water heating. Int J Refrig 28, 1064–1072. doi:10.1016/j.ijrefrig.2005.03.004

Ituna-Yudonago, J.F., Belman-Flores, J.M., Elizalde-Blancas, F., Garcï¿½a-Valladares, O., 2017.

This is the accepted version of an article published in Thermal Science and Engieering Progress
http://dx.doi.org/10.1016/j.tsep.2020.100590

Numerical investigation of CO2behavior in the internal heat exchanger under variable boundary conditions of the transcritical refrigeration system. Appl Therm Eng 115, 1063–1078. doi:10.1016/j.applthermaleng.2017.01.042

Kim, M.H., Pettersen, J., Bullard, C.W., 2004. Fundamental process and system design issues in CO2 vapor compression systems. Prog Energy Combust Sci 30, 119–174. doi:10.1016/j.pecs.2003.09.002

Kim, Mo Se, Kang, D.H., Kim, Min Soo, Kim, M., 2017. Étude de la régulation optimale de la pression du refroidisseur de gaz pour un système frigorifique au CO2avec un échangeur de chaleur interne. Int J Refrig 77, 48–59. doi:10.1016/j.ijrefrig.2017.03.002

Liu, F., Groll, E. a., 2013. Study of ejector efficiencies in refrigeration cycles. Appl Therm Eng 52, 360–370. doi:10.1016/j.applthermaleng.2012.12.001

Lorentzen, G., 1994. Revival of carbon dioxide as a refrigerant. Int J Refrig 17, 292–301. doi:10.1016/0140-7007(94)90059-0

Milazzo, A., Mazzelli, F., 2017. Future perspectives in ejector refrigeration. Appl Therm Eng 121, 344–350. doi:10.1016/j.applthermaleng.2017.04.088

Minetto, S., Brignoli, R., Zilio, C., Marinetti, S., 2014. Experimental analysis of a new method for overfeeding multiple evaporators in refrigeration systems. Int J Refrig 38, 1–9. doi:10.1016/j.ijrefrig.2013.09.044

Nakagawa, M., Marasigan, A.R., Matsukawa, T., 2011. Experimental analysis on the effect of internal heat exchanger in transcritical CO2 refrigeration cycle with two-phase ejector. Int J Refrig 34, 1577–1586. doi:10.1016/j.ijrefrig.2010.03.007

Rigola, J., Ablanque, N., Pérez-Segarra, C.D., Oliva, A., 2010. Numerical simulation and experimental validation of internal heat exchanger influence on CO2 trans-critical cycle performance. Int J Refrig 33, 664–674. doi:10.1016/j.ijrefrig.2009.12.030

Sawalha, S., 2008. Carbon Dioxide in Supermarket Refrigeration.

Sawalha, S., Karampour, M., 2015. Field measurements of supermarket refrigeration systems . Part I : Analysis of CO 2 trans-critical refrigeration systems 87, 633–647. doi:10.1016/j.applthermaleng.2015.05.052

Shariatzadeh, O.J., Abolhassani, S.S., Rahmani, M., Nejad, M.Z., 2016. Comparison of transcritical CO2 refrigeration cycle with expander and throttling valve including/excluding internal heat exchanger : Exergy and energy points of view. Appl Therm Eng 93, 779–787.

This is the accepted version of an article published in Thermal Science and Engieering Progress
http://dx.doi.org/10.1016/j.tsep.2020.100590

doi:10.1016/j.applthermaleng.2015.09.017

Sharma, V., Fricke, B., Bansal, P., 2014. Comparative analysis of various CO2 configurations in supermarket refrigeration systems. Int J Refrig 46, 86–99. doi:10.1016/j.ijrefrig.2014.07.001

Singh, S., Dasgupta, M.S., 2017. CO 2 heat pump for waste heat recovery and utilization in dairy industry with ammonia based refrigeration. Int J Refrig 78, 108–120. doi:10.1016/j.ijrefrig.2017.03.009

Taylor, B.N., Kuyatt, C.E., 2001. Guidelines for Evaluating and Expressing the Uncertainty of NIST Measurement Results. Natl Inst Stand Technol Gaithersburg, MD D.1.1.2.

Taylor, P., House, M., Street, M., Wt, L., Groll, E.A., Kim, J., 2007. Review of Recent Advances toward Transcritical CO2 Cycle Technology. HVAC&R Res 13, 499–520.

Torrella, E., Sánchez, D., Llopis, R., Cabello, R., 2011. Energetic evaluation of an internal heat exchanger in a CO2 transcritical refrigeration plant using experimental data. Int J Refrig 34, 40–49. doi:10.1016/j.ijrefrig.2010.07.006

This is the accepted version of an article published in Thermal Science and Engieering Progress
http://dx.doi.org/10.1016/j.tsep.2020.100590